Proceedings of ASME Eighth International Conference of

Fluid Dynamics and Propulsion

December 14 - 17, 2006, Sharm el Sheikh, Sinai, Egypt

ICFDP8-EG-149

A MATHEMATICAL MODEL FOR MAGNETO-RHEOLOGICAL DAMPERS SUBJECTED TO SINUSOIDAL EXCITATION

Hany A. Gomaa
E. Saber
H. El-Gamal

Arab Academy for Science, Technology and Maritime Transport

ABSTRACT

Semi active control devices received significant attention because they offer the adaptability of active control devices without requiring associated large power sources. Magnetorheological dampers, or as they are more commonly called MR dampers are a kind of semi-active controlled devices that are being developed for a wide variety of applications where controllable damping is desired. These applications include dampers for automobiles, heavy trucks, bicycles, prosthetic limbs, gun recoil systems, robot control and many others. The objective of this work is to obtain a time dependent mathematical model that can clearly describe the MR fluid behavior while the damper is subjected to a sinusoidal excitation.

Key words: Semi-active control devices, MR dampers, MR fluid.

INTRODUCTION:

Due to the increased applications and usages of the MR dampers in many engineering fields a demand to better understand their behavior has been rising tremendously. The performance of an MR damper depends mainly on the properties of the MR fluid used in it. Spencer et al [1] proposed an improved mechanical model for an MR damper that overcame some drawbacks and inadequacy of the other models, especially in the cases were the velocity and acceleration have opposite signs and the magnitude of the velocities were very small. Kelso's [2] work included a characterization of a prototype MR damper that provides consistent controllability of damping throughout the current range. Spencer et al [3] examined the efficiency of various models for prediction of the response of full-scale MR dampers. They studied and compared the prediction ability of both axi-symmetric model and a simpler approximated parallel plate model. Yang et al [4] designed and constructed a 200kN MR damper that is capable of providing semi-active damping for full-scale structural applications. Spencer et al [5] carried out experiments and analytical work on a two degree of freedom model for design control during which they assumed a linear behavior of the MR damper which was not accurate especially with a smart damping device such as MR damper that have highly non linear characteristics. Lederer et al [6] showed that the theoretical modeling of the MR damper behavior can give the mathematical structure only, while the model parameters depend mainly on the MR-fluid and damper construction. Giua et al [7] showed a procedure for the design of a semi-active suspension, to be applied, to road vehicles with MR-dampers. Calderón et al [8] studied theoretically the dynamics of a system of two magnetically active particles suspended in a non-magnetic fluid subjected to a rotating magnetic field. Dyke et al [9] proposed a type of clipped-optimal controller based on acceleration feedback. They demonstrated the effectiveness of the MR damper using the proposed clipped-optimal control law through a numerical example. Barroso et al [10] presented a quasi-controller for a non-linear structure and displayed its efficiency in simulation against suites of several earthquakes of near and far field origin and intensity. Umit et al [11] presented a full damper

design that can be used to lower the vibrations from exceeding certain limits in vehicular applications. Godaninejad et al [12] presented experimental and theoretical studies on heat generation and dissipation of field-controllable magneto-rheological (MR) fluid shock absorbers. Breese et al [13] presented the development and evaluation of field-controllable, semi-active fail-safe magneto-rheological fluid (MRF) damper for mountain bicycle. The aim of the present work is to take a second step in studying the behavior of the MR dampers, especially those subjected to sinusoidal excitations, by taking the unsteady flow nature of the damper into account.

1. ANALYSIS:

Figure (1) describes the MR damper geometry and variables used in the analysis. The annular gap (i.e. the distance between the piston and the cylinder inner housing) is represented by h on the figure. Assuming that the flow is unsteady, fully developed (i.e., neglecting the entrance and exit effects), incompressible, isoviscous and laminar. Then the flow in the damper is therefore governed by the momentum equation,

$$\rho\frac{\partial}{\partial t}u\,(r)-\frac{\partial}{\partial r}\tau_{rx}(r)-\frac{\tau_{rx}(r)}{r}=-\frac{\partial p}{\partial x} \tag{1}$$

Where, $u\,(r)$ is the flow velocity in the longitudinal direction, $\tau_{rx}(r)$ is the shear stress, and $\frac{\partial p}{\partial x}$ is the pressure gradient.

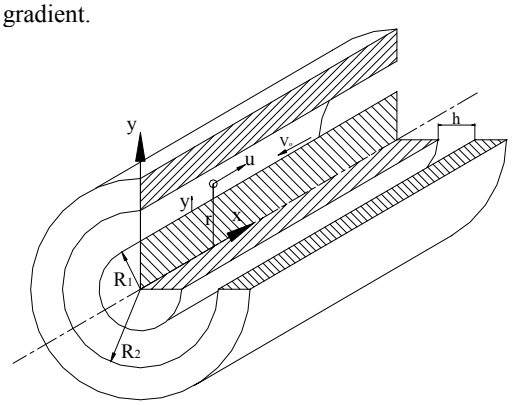

Figure1. Damper geometry and co-ordinate system, (sectioned for clarity)

A simple Bingham model is used to describe the essential field dependent fluid characteristics.
The stress rate of strain relationship may be written as,

$$\tau=\tau_0\,\mathrm{sgn}\left(\frac{\partial u}{\partial r}\right)+\mu\left(\frac{\partial u}{\partial r}\right),\ |\tau|>|\tau_0| \tag{2}$$

$$\dot{\gamma}=\frac{\partial u(r)}{\partial r}=0,\ |\tau|<|\tau_0| \tag{3}$$

$$\rho\frac{\partial u}{\partial t}-\mu\frac{\partial^2 u}{\partial y^2}-\frac{1}{(R_1+y)}\tau_0(H)\mathrm{sgn}\left(\frac{\partial u}{\partial y}\right)-\frac{1}{(R_1+y)}\mu\frac{\partial u}{\partial y}=-\frac{\partial p}{\partial x} \tag{4}$$

Substituting from 2 into 1 and letting r=R_1+y, we get
For simplicity, the curvature effect of the damper surface is to be neglected and equation (4) becomes,

$$\frac{\partial u}{\partial t}-\nu\frac{\partial^2 u}{\partial y^2}=-\frac{1}{\rho}\frac{\partial p}{\partial x} \tag{5}$$

Assuming that the velocity has the following sinusoidal form:
$u(y,t)=U_0\Phi(y)e^{int}$,Where Φ is a complex variable,
let $\Phi(y)=\phi(y)+i\theta(y)$,then $u(y,t)=U_0\,\phi\,e^{int}+iU_0\theta e^{int}$

And also let $\frac{\partial p}{\partial x}=Pe^{\mathrm{int}}$,where P is a real quantity
Substituting into equation (5) , we have

$$inU_0\phi-nU_0\theta-\nu U_0\left(\phi''+iU_0\theta''\right)=-\frac{1}{\rho}P$$

Separating real and imaginary parts yields,

$$\phi''=\frac{P}{\mu U_0}-\frac{n}{\nu}\theta \tag{6}$$

$$\theta''=\frac{n}{\nu}\phi \tag{7}$$

where the primes denote differentiation with respect to y.
Introducing the following dimensionless variables:

$$y^*=\frac{y}{h},\qquad t^*=nt,\qquad p^*=\frac{p}{(\mu U_0/h)}$$

$$x^*=\frac{x}{L},\qquad P^*=\frac{P}{\left(\frac{\mu U_0}{hL}\right)}=\frac{P}{\left(\frac{\mu U_0}{h^2}\right)\left(\frac{h}{L}\right)}\ \text{and}$$

$$\frac{\partial p^*}{\partial x^*}=P^*e^{it^*}$$

Substituting these dimensionless variables, into equations (6) and (7) we get,

$$\frac{d^2\phi}{dy^{*2}}=\left(\frac{h}{L}\right)P^*-\mathrm{Re}\,S\theta \tag{8}$$

$$\frac{d^2\theta}{dy^{*2}}=\mathrm{Re}\,S\phi \tag{9}$$

Where $\mathrm{Re}=\frac{U_0h}{\nu}$ and $S=\frac{nh}{U_0}$ (Re is the Reynolds number and S is the Strouhal number)
The boundary condition on the piston wall is,
y=0 , u = $V_0\,e^{int}$

That is $\phi(0) = V_0^* = \frac{V_o}{U_o}$, and $\theta(0) = 0$

On the cylinder wall, y = h and u = 0

And therefore , ϕ (h) = 0 and θ(h)= 0.

Figure 2 provides typical Bingham plastic shear flow regions in the annular gap. In regions I and II, the shear stress has exceeded the yield stress and the fluid flows. In region III, the shear stress is lower than the yield stress, so no shear flow occurs, this is often referred to as the plug flow region.

Region III or the plug flow region is seen to be bounded between y_1 and y_2. In this region the flow velocity is constant because the shear stress is less than the yield stress.

$$\dot{\gamma} = \frac{\partial u}{\partial y} = 0$$

That is, $\phi' = 0$ and $\theta' = 0$ for $\left(y_1 \le y \le y_2\right)$

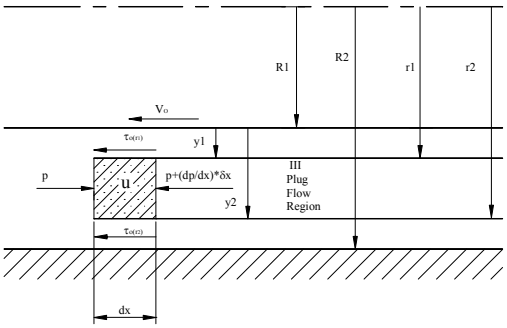

Figure 2 The plug flow region and free body diagram of MR flow through it

Using the free body diagram of the MR fluid in the plug region shown on figure 2, we also have

$$\rho\frac{\partial u}{\partial t}\pi\left(r_2^2 - r_1^2\right)dx = -\frac{\partial p}{\partial x}dx\pi\left(r_2^2 - r_1^2\right) + 2\pi r_1 dx\tau_0 + 2\pi r_2 dx\tau_0$$

$$r_2 - r_1 = \frac{2\tau_0}{\text{Real}\left[\frac{\partial p}{\partial x} + \rho\frac{\partial u}{\partial t}\right]}$$

That is, $$y_2 - y_1 = \frac{2\tau_0}{\text{Real}\left[\frac{\partial p}{\partial x} + \rho\frac{\partial u}{\partial t}\right]}$$

And since the velocity in the plug flow region is constant then,

$$y_2 - y_1 = \frac{2\tau_0}{\text{Real}\left[Pe^{\text{int}} + \rho U_0 in\left[\phi(y_1) + i\theta(y_1)\right]e^{\text{int}}\right]}$$

$$y_2 - y_1 = \frac{2\tau_0}{C\cos nt - D\sin nt}$$

where $C = P - n\rho U_o\theta(y_1)$ and $D = n\rho U_o\phi(y_1)$

In dimensionless form we may write,

$$y_2^* - y_1^* = \frac{2\tau_0^*}{C^*\cos t^* - D^*\sin t^*} \tag{10}$$

With $C^* = \left(\frac{h}{L}\right)P^* - \text{Re}\,S\theta\left(y_1^*\right)$ and $D^* = \text{Re}\,S\phi\left(y_1^*\right)$

By applying the fluid continuity consideration we may write,

$$q = \int_{R_1}^{R_2} u\left(2\pi r dr\right) = 2\pi U_0\int_0^h \left(R_1 + y\right)\left[\phi\cos nt - \theta\sin nt\right]dy \tag{11}$$

Introducing the dimensionless variables into the equation yields,

$$q = 2\pi U_0 R_1 h\int_0^1\left[1 + y^*\left(\frac{h}{R_1}\right)\right]\left[\phi\cos t^* - \theta\sin t^*\right]dy^*$$

$q = \pi R_1^2 V_0\cos nt$ where R_1 is the piston radius, and therefore the dimensionless piston velocity becomes,

$$V_0^* = \frac{V_0}{U_0} = 2\left(\frac{h}{R_1}\right)\frac{1}{\cos t^*}\int_0^1\left[1 + y^*\left(\frac{h}{R_1}\right)\right]\left[\phi\cos t^* - \theta\sin t^*\right]dy^* \tag{12}$$

An approximate solution for the case when Re*S* is very small is required during the iteration process for solving equations (6) and (7) numerically in order to provide initial guesses for the extent of the plug region inside the solution domain. After simplification equations (8) and (9) become,

$$\frac{d^2\phi}{dy^{*2}} = \left(\frac{h}{L}\right)P^* \tag{13}$$

and $$\frac{d^2\theta}{dy^{*2}} = 0 \tag{14}$$

With $\phi(0) = V_0^*$ and $\theta(0) = 0$ } region I

$\phi'(y_1^*) = 0$ and $\theta'(y_1^*) = 0$ } region I

$\phi'(y_2^*) = 0$ and $\theta'(y_2^*) = 0$ } region II

$\phi(1) = 0$ and $\theta(1) = 0$ } region II

Therefore a trivial solution for θ exists that is, θ = 0

Integrating equation 13 twice with respect to y^*, and using the boundary conditions in region I we have,

$$\phi = \frac{1}{2}\left(\frac{h}{L}\right)P^*\left(y^{*2} - 2y_1^* y^*\right) + V_0^* \tag{15}$$

Equation 13 also holds for region II and substitution of the boundary conditions yields,

$$\phi = \frac{1}{2}\left(\frac{h}{L}\right)P^*\left(y^{*2} - 2y_2^* y^* + 2y_2^* - 1\right) \tag{16}$$

But in the plug region $\phi' = 0$

That is, $\phi(y_1^*) = \phi(y_2^*)$

And therefore,

$$y_2^{*2} - 2y_2^* - y_1^{*2} + 1 = \frac{-V_0^*}{\frac{1}{2}\left(\frac{h}{L}\right)P^*} \tag{17}$$

From equations (17) and (10) we may write,

$$y_1^* = y_2^* - \frac{2\tau_0^*}{\left(\frac{h}{L}\right)P^*\left|\cos t^*\right|} \tag{18}$$

Substituting from (18) into (17) we get,

$$y_1^* + y_2^* - 1 = \frac{2V_0^*\left|\cos t^*\right|}{\left(\frac{h}{L}\right)P^*\left|\cos t^*\right| - 2\tau_0^*} \tag{19}$$

From (18) and (19) we get,

$$y_2^* = \frac{\tau_0^*}{\left(\frac{h}{L}\right)P^*\left|\cos t^*\right|} + \frac{V_0^*\left|\cos t^*\right|}{\left(\frac{h}{L}\right)P^*\left|\cos t^*\right| - 2\tau_0^*} + \frac{1}{2} \tag{20}$$

2. SOLUTION PROCEDURE:

Initially the force is given as an input having a sinusoidal cosine form. Then using equation (12) V_o^* is found at any chosen time. The following step is to obtain the relation ship between the piston velocity and the input force. Using the force velocity relationship and giving the piston a sinusoidal velocity signal the damping force versus time relationship is now known. By simple integration of the piston velocity over the time domain, the displacement at each time is found. Then using equations (18) and (20) to find y_1*and y_2* respectively, the plug flow region extent is found at every time t.

3. RESULTS AND DISCUSSION:

A case study of a 200 kN MR damper, used in civil engineering application for reducing the effect of vibration on structures, is presented and compared with the results obtained experimentally for a similar damper using the same MR fluid type. Moreover, a comparison is made between theoretically obtained results, by Spencer [1], using the same mechanical model (the Bingham model) and present model results. In addition, for generality purpose, an additional comparison between the experimental results available for the MRD-1005-3 damper, used in car applications and those of the present model are made. These comparisons together with the case study are made in order to verify the correctness of the present theoretical approach and the numerical procedure considered.
The MR fluid chosen for the application of the theoretical model is the MRX-145-2BD. This type of MR fluid is mainly used to work inside large scale MR dampers for its large yield stress created upon the input of small current intensities to the damper. The relationship between the yield stress and the input current, for this fluid, is shown in figure 3.

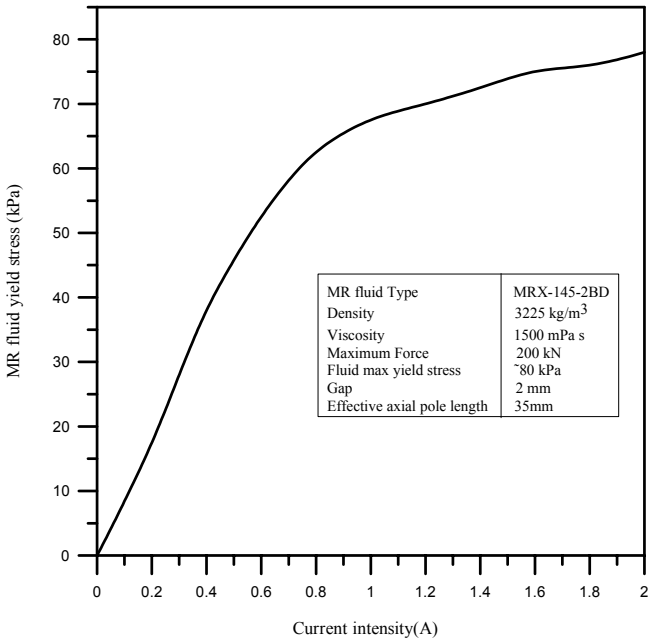

FIGURE 3 THE YIELD STRESS AGAINST THE CURRENT INTENSITY FOR THE MRX-145-2BD TAKEN FROM REFERENCE [13]

The response of the 200 kN MR damper due to an 0.5 Hz sinusoidal excitation is shown in figures 4 through 10 for constant input currents of 0 , 0.25, 0.5, 0.75, 1, 1.5 and 2 A respectively. In all the figures, the effects of changing the magnetic field, corresponding to changing of the input current intensity, are readily observed. At zero current the MR damper primarily exhibits the characteristics of a purely viscous device (i.e., the force-displacement relationship is approximately elliptical, and the force-velocity relationship is nearly linear). However, as the current increases, the force required to yield the MR fluid in the damper increases and produces behavior associated with a plastic material in parallel with a viscous damper (i.e. the Bingham plastic behavior) .
Figure 4 shows the damping force against the piston displacement for an input current range from 0A to 2A. It is noticed that the largest displacement traveled by the piston

was made at the zero current input, about 60 mm , and as the current increases the displacement decreases until reaching about 25 mm for an input current intensity of 2 A. This is due the additional resistance to motion with the same speed range at the increased current inputs. Similarly figure 5, shows the relationship between the MR fluid damping force against the piston velocity. At zero current intensity the relationship is almost linear as if a Newtonian fluid is used for damping but as the current increases the Bingham model plastic effect is shown to affect the characteristics considerably. Also, as the velocity decreases and before it changes sign, the force-velocity relationship is no longer linear and decreases sharply.

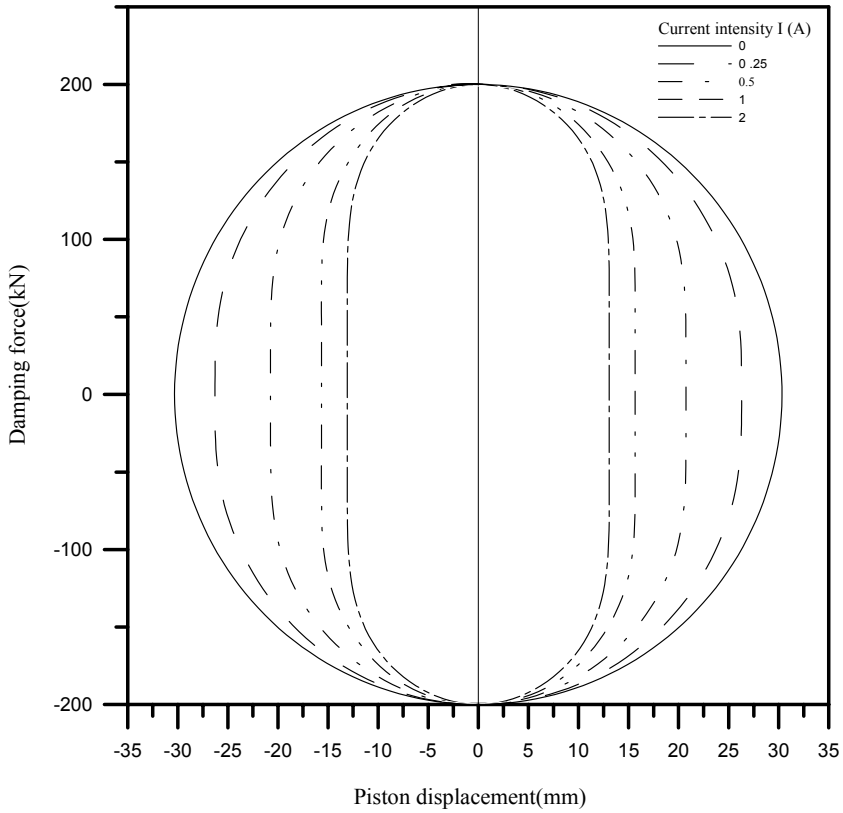

FIGURE 4 THE DAMPING FORCE VERSUS PISTON DISPLACEMENT AT DIFFERENT INPUT CURRENT INTENSITIES

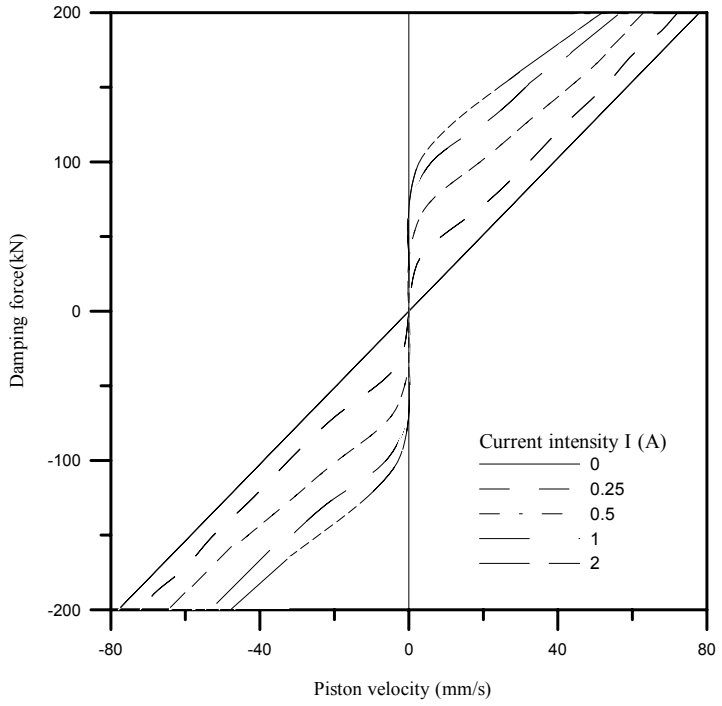

FIGURE 5 THE DAMPING FORCE VERSUS DAMPER PISTON VELOCITY AT DIFFERENT INPUT CURRENT INTENSITIES

Moreover figure 6 shows the plug flow region thickness against time for different current intensities. The curves show the effect of increasing the current intensity on the plug region thickness. It is seen that as the current increases the extent plug flow region increases until the whole region almost turns into a plug flow region , showing complete solid like effect at the highest allowable current intensity of 1.5A or 2 A , where almost the whole fluid is magnetized into chain like structures. However at zero current, no plug flow region exists except instantaneously when the piston comes to rest upon changing its direction of movement after 0.5 s of starting its motion. Note that the rate of change of the thickness of the plug flow region at small values of the current intensities is higher than the rate of change found at large values of current intensities. And in order to monitor the effect of current increase on the velocity profile, the velocity distribution at the same time interval of $t=\frac{1}{3}$ s or $t=\frac{1}{3}\pi$ radians are plotted against the position, y in mm, at different current intensities in figure 7. It is clearly seen that as the current increase the velocity profile at the same time interval gets flatter as the plug flow region gets thicker. It should also be noted that at y=0, the velocity of the fluid equals the piston rod velocity, satisfying the no slip condition. In order to study the effect of changing the operating frequency on the behavior of the MR damper figure 8 shows the damping force against piston's velocity for a constant 1 A current input for different frequencies. The frequencies considered are 0.5, 1, 2, 5, 10, 20, 40 and 50 Hz respectively. The results show that the change of frequency does not have any noticeable effect on the output data. This is in agreement with all previous conclusions made by previous investigators suggesting that the change of frequency has a negligible effect on the obtained results.

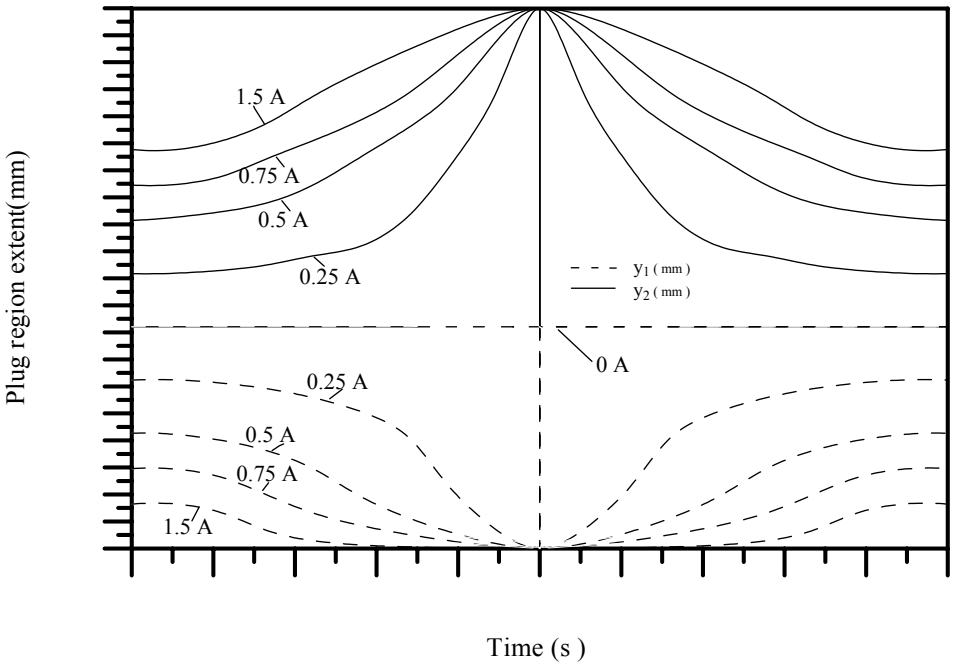

FIGURE 6 THE PLUG REGION EXTENT AGAINST THE TIME FOR DIFFERENT VALUES OF INPUT CURRENT INTENSITIES

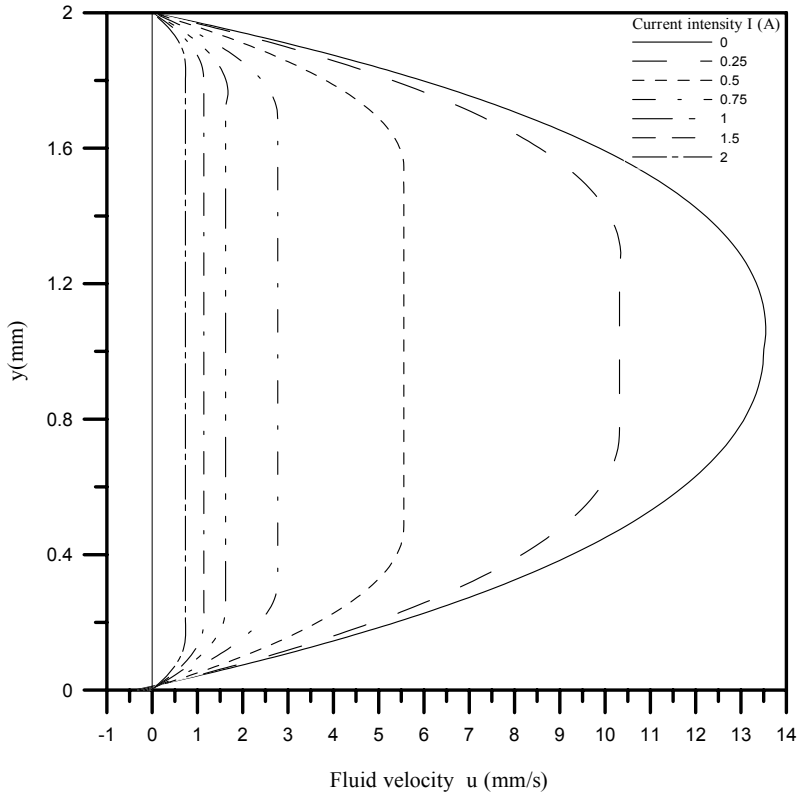

FIGURE 7 FLUID VELOCITY PROFILES AT DIFFERENT CURRENT INTENSITIES AND TIME INTERVAL T= $\frac{1}{3}$ S OR T= $\frac{1}{3}\ \pi$ RADIANS

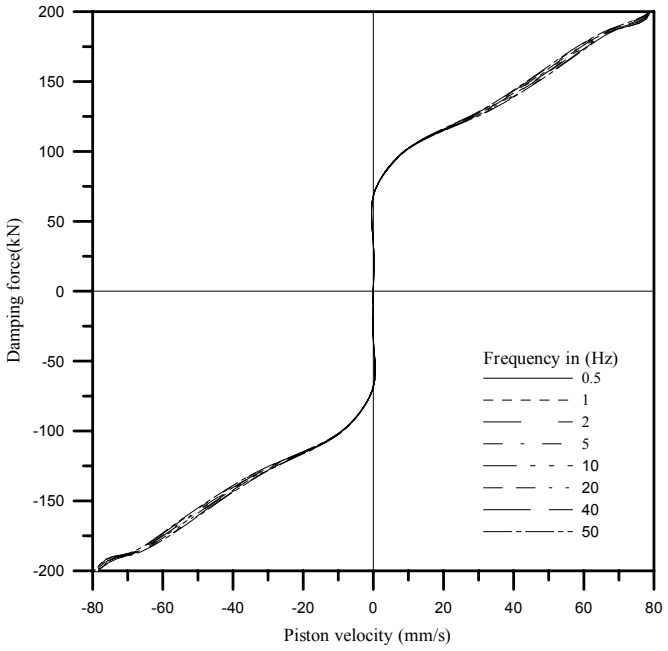

FIGURE 8 THE DAMPING FORCE VS. THE DAMPER PISTON VELOCITY AT DIFFERENT INPUT FREQUENCIES AT A CONSTANT INPUT CURRENT INTENSITY OF 1A

For the sake of comparison between the present results and those theoretically obtained by Yang [13] for a similar damper configuration and using the same type of MR fluid, they are plotted together in figures 9a and 9b. Figure 9a shows the damping force against the piston velocity for both results at the same input current intensity of 1A. Although the theoretical results exhibit a hysteresis behavior unlike the present results, they show some qualitative agreement. Figure 9b shows the relationship between the damping force in (kN) and the piston displacement in (mm) again for the same input current intensity of 1A. Good agreement is obtained.

Additional comparisons between the present theoretical model and previously proposed Bingham model by Spencer

[1] are also given in figures 10a and 10b. Although the present theoretical model results are taken for an MR fluid different from that used in the mechanical models of reference [1], qualitative agreement are found with previously proposed Bingham model.

An important and commonly used type of MR damper is the MRD-1005-3 which is used in certain car models. And to extend comparisons to cover a wider range of applications, additional comparisons between experimental data obtained for that damper [14] and the present results are made and plotted in figures 11a and 11b. Again, although the MRD - 1005-3 damper has a different type of MR fluid, the three figures show good qualitative agreement between all obtained results, at the same input current intensity of 0.5 A.

(a)

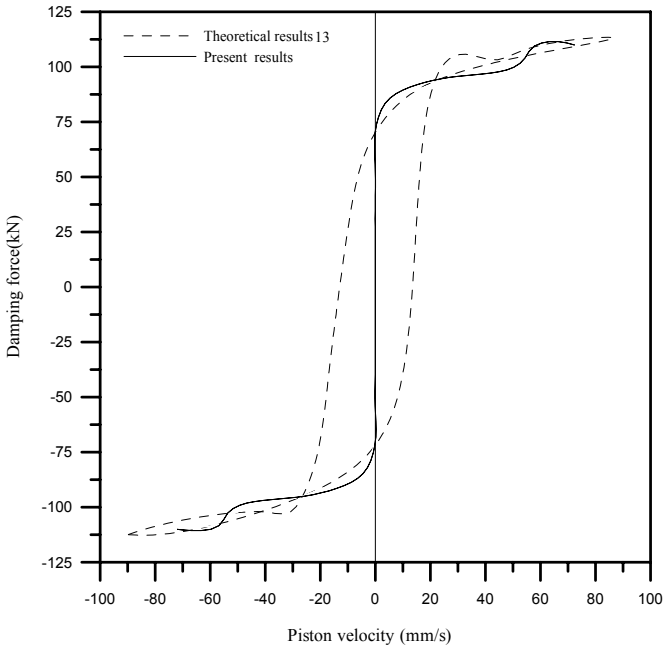

(b)

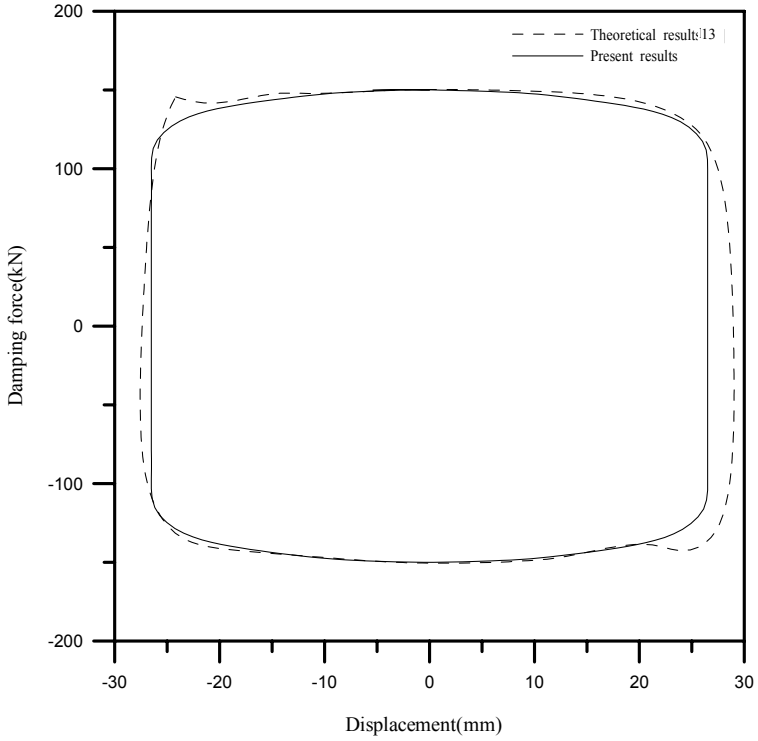

FIGURE 9 COMPARISONS BETWEEN THE PRESENT RESULTS AND THOSE OF REFERENCE [13] FOR AN INPUT CURRENT INTENSITY OF 1A.
A) THE DAMPING FORCE VERSUS PISTON VELOCITY
B) THE DAMPING FORCE VERSUS PISTON DISPLACEMENT

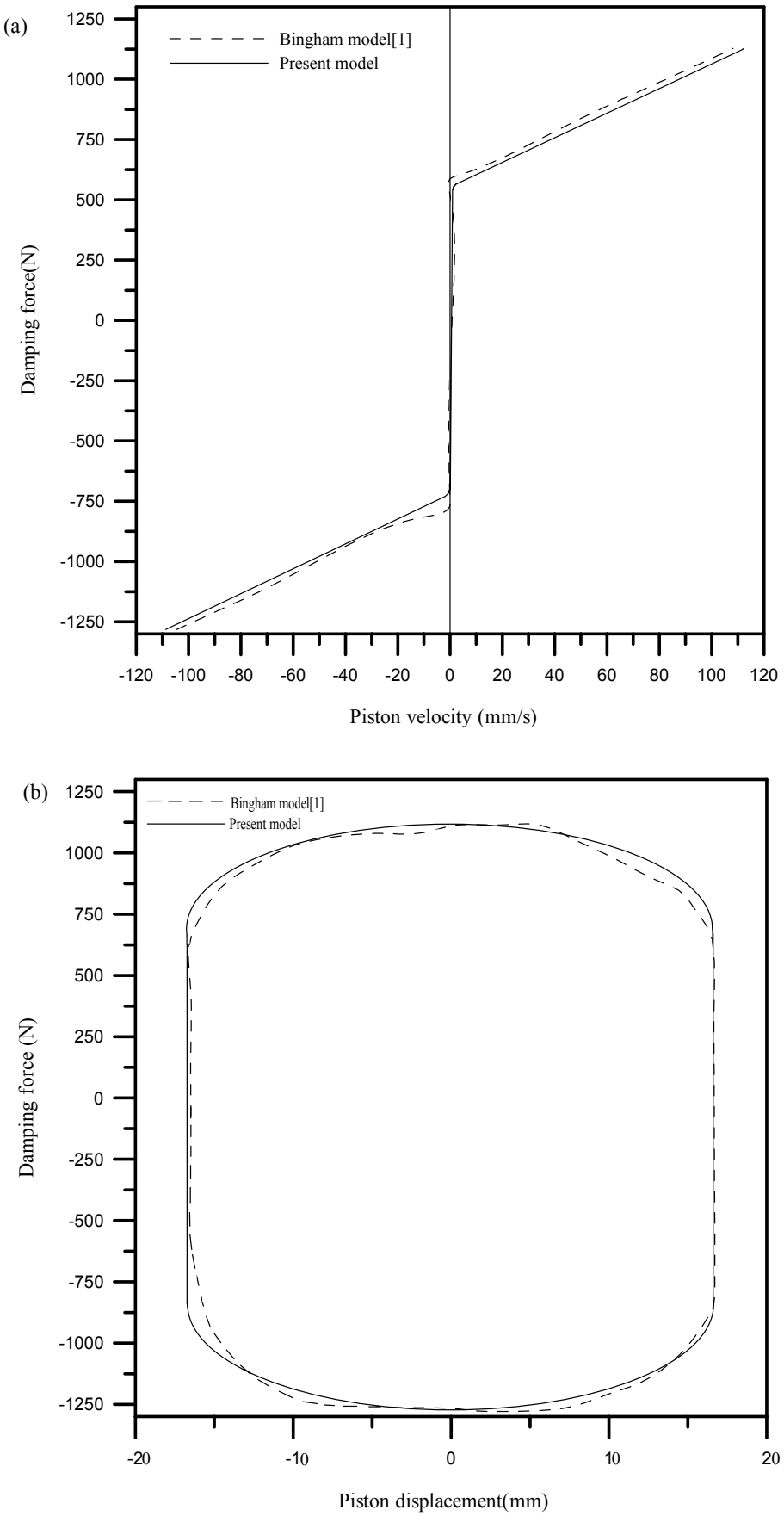

FIGURE 10 COMPARISON BETWEEN THE PRESENT RESULTS AND THE BINGHAM MODEL PRESENTED IN REFERENCE [1].
(A) THE DAMPING FORCE VERSUS PISTON VELOCITY
(B) THE DAMPING FORCE VERSUS PISTON DISPLACEMENT

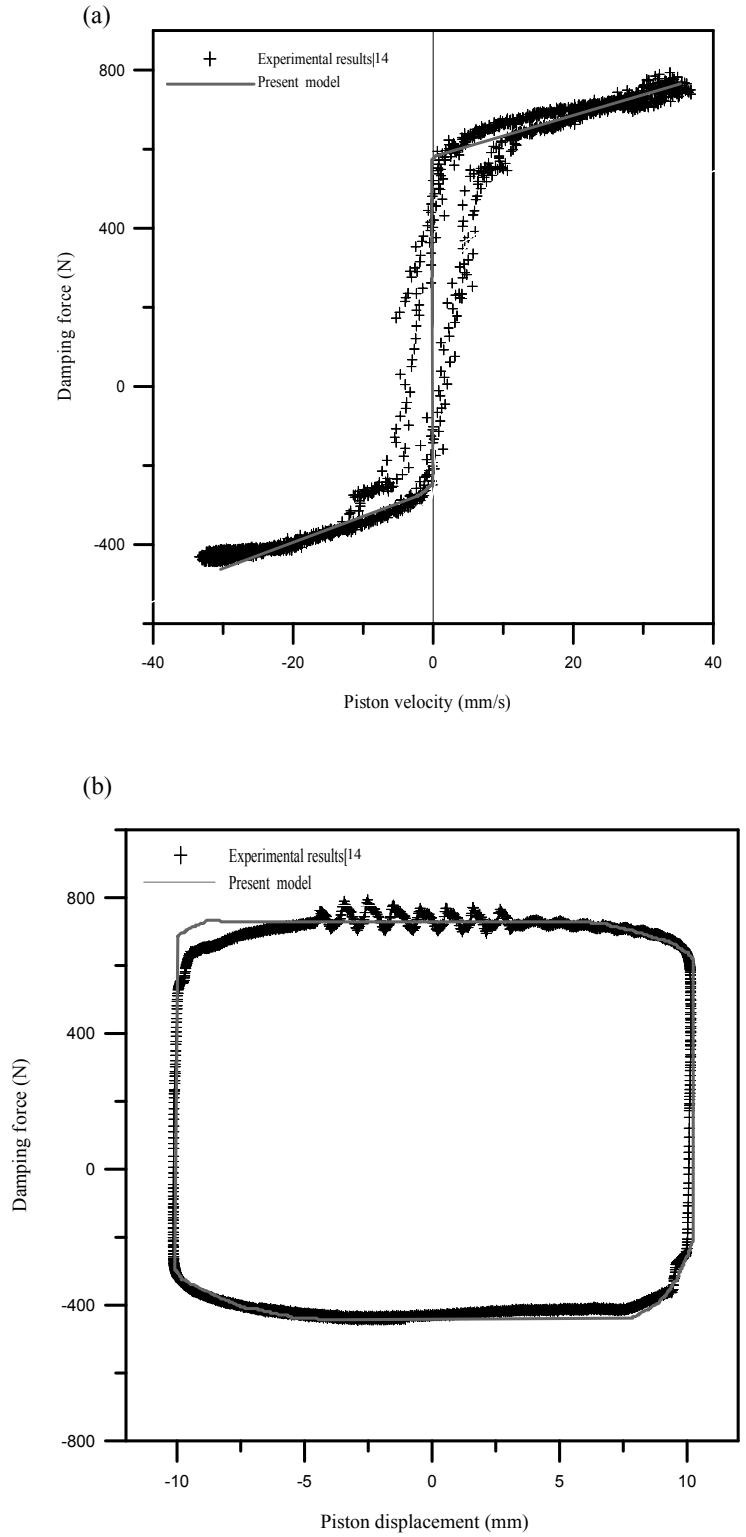

FIGURE 11 COMPARISON BETWEEN THE PRESENT RESULTS AND THE EXPERIMENTAL RESULTS OF REFERENCE [14] FOR INPUT CURRENT INTENSITY OF 0.5 A.
A) THE DAMPING FORCED VERSUS PISTON VELOCITY
B) THE DAMPING FORCE VERSUS PISTON DISPLACEMENT

5. CONCLUSIONS:

The model presented in this paper proved that it can clearly describe the MR fluid behavior while the MR damper is in operation under a sinusoidal excitation. The model is characterized by having the ability to be applied on different MR dampers, used for many applications, and on many different kinds of MR fluids under the conditions that the MR damper geometry and MR fluid properties are all known.

6. NOMENCLATURE:

n	frequency number	(1/s)
p	the pressure amplitude	(Pa)
q	volume flow rate	(m^3/s)
r	radial coordinate (radial distance measured from the center line of the piston)	(mm)
R_1	represents the piston radius	(mm)
R_2	represents the cylinder inner housing radius	(mm)
Re	the Reynolds number $\mathrm{Re} = \frac{U_0 h}{\nu}$	
S	the Strouhal number $S = \frac{nh}{U_0}$	
Sgn	+ve or –ve	
u	flow velocity	(m/s)
x	longitudinal coordinate	(mm)
y	the coordinate in the radial direction normal to the solid boundary	(mm)

Greek symbols

$\dot{\gamma}$	shear strain rate	(1/s)
μ	is the viscosity of the MR fluid (found in the gap)	(kg/ms)
ν	the kinematic plastic viscosity $\nu = \frac{\mu}{\rho}$	(m^2/s)
ρ	fluid density	(kg/m^3)
τ	total shear stress	(Pa)
τ_0	yield stress caused by the applied field	(Pa)

7. REFERENCES:

[1] Spencer, B. F., Dyke, S. J., Sain, M. K. and Carlson, J. D, "Phenomenological model of a magneto-rheological damper", ASCE Journal of Engineering Mechanics, vol.123, pp.230-238, 1997

[2] Kelso S. P. "Experimental characteristics of commercially practical magneto-rheological fluid damper technology", Proceedings of SPIE Conference on Smart Structures and Materials, Paper No. 4332–34, New Port Beach, CA, March, 2001

[3] Spencer, B. F., Yang, G., Carlson, J. and Sain, M.K , "Smart dampers for seismic protection of structures: a full-scale study.", Proceedings of the Second World Conference on Structural Control, Kyoto, Japan, June 28 – July 1, 1998.

[4] Yang G., Spencer, B.F., Carlson, J.D., and Sain, M.K, "Large-scale MR fluid dampers: Modeling and dynamic performance considerations," Engineering Structures, vol. 24, no. 3, pp. 309-323, March 2002.

[5] Spencer, B.F. , Yoshioka, H., and Ramallo, J. C., M.K, Smart base isolation strategies employing magneto-rheological dampers", Journal of engineering mechanics , 128(5): 540-551, 2002.

[6] Lederer, P., Salloker, M.G., and Doczy, S, Modeling of a magnetorheological damper by parameter-estimation, Proceedings of the 7th International Conference on New Actuators, Bremen, Germany, pp. 143-146, 2000

[7] Giua, A., Melas, M., and Seatzu, C, "Design of a control law for a magneto- rheological suspension," Proceeding of the European Control Conference 2003 Cambridge, UK, Sep 2003.

[8] Calderón, O. G., and Melle , S, "Dynamics of simple magneto-rheological suspensions under rotating magnetic fields with modulated Mason number" J. Phys. D: Appl. Phys. 35 2492-2498. Volume 35, No 20, 21 October 2002.

[9] Dyke, S. J., Spencer, B. F., Sain, M. K. and Carlson, J. D, "Modeling and control of magneto-rheological dampers for seismic Response Reduction," Smart Materials and Structures, No5, pp. 565-575, 1996.

[10] Barroso, L. R., Hunt, S., and Chase, J. G,"Application of magneto-rheological dampers for multi-level seismic hazard mitigation of hysteretic structures', proceedings of the 15th ASCE Engineering Mechanics Conference, June 2-, Columbia University , New York, NY,5,2002.

[11] Umit, D.,and Cahit A .A new magneto-rheological fluid damper for high mobility multi-purpose wheeled vehicle (HMMWV). Smart Structures and Materials 2003: Damping and Isolation. Edited by Agnes, Gregory S.; Wang, Kon-Well. Proceedings of the SPIE conference, on smart material and structure, vol. 5052, pp. 198-206, 2003.

[12] Gordaninejad, F., and Bresse, D. G., Heating of Magnetorheological fluids

dampers. University of Nevada, Composite and Intelligent Materials Laboratory. Proc. SPIE conference of Smart Structures and Materials .Vol. 3671, p. 2-10, 05/1999

[13] Breese, D. J., and Gordaninejad, F, "Semi-active, fail-safe magneto-rheological fluid dampers for mountain bicycles", International Journal of Vehicle Design, Vol.33, Nos.1/2/3/, pp.138-152, 2003.

[14] Yang, G., "Large scale magnetorheological fluid damper for vibration mitigation, modeling, testing and control", PhD dissertation, Department Of Civil Engineering And Geological Sciences, University of Notre Dame, Indiana, December 2001.

[15] Ang,W.L, Li, W.H.and Du,H., "Experimental and modeling approaches of a MR damper performance under harmonic loading", The Journal of the Institute Of Engineers, Singapore, vol.44, Issue 4 , 2004.